Theriogenology 227 (2024) 112–119

Contents lists available at ScienceDirect

Theriogenology

journal homepage: www.theriojournal.com

# Densitometric analysis of GnRH and IBA1 immunocytochemistry in the basal ventromedial hypothalamus of the ewe

M. Merchán Jr. [a], I. Plaza [b], J. Nieto [a], J. Plaza [a], J.A. Abecia [c], C. Palacios [a,*]

[a] Animal Production Area, Department of Construction and Agronomy, Faculty of Agricultural and Environmental Sciences, University of Salamanca, Avda. Filiberto Villalobos, 119, 37007, Salamanca, Spain
[b] Auditory Neuroplasticity Laboratory, Institute for Neuroscience of Castilla y León (INCYL), University of Salamanca. Salamanca. Calle del Pintor Fernando Gallego, 2, 37007, Spain
[c] IUCA. Departamento de Producción Animal y Ciencia de los Alimentos, Universidad de Zaragoza, Miguel Servet, 177, 50013, Zaragoza, Spain

ARTICLE INFO

*Keywords:*
Microglia
Independent component analysis
Seasonal hypothalamic activation
Churra Ewe

ABSTRACT

Gonadotropin releasing hormone (GnRH) synthesis and secretion regulates seasonal fertility. In the brain, the distribution of GnRH-positive neurons is diffuse, hindering efforts to monitor variations in its cellular and tissue levels. Here, we aim at assessing GnRH immunoreactivity in nuclei responsible for seasonal fertility regulation (SFR) within the posterior, anterior, and preoptic areas of the basal hypothalamus during estrous in ewes. We detected reaction products in the ventromedial basal hypothalamus in neurons, nerve fibers, non-neuronal immunoreactive bodies, and diffuse interstitial areas. Immunoreactivity correlated with the distribution of the main SFR nuclei in the arcuate, retrochiasmatic, periventricular, medial preoptic, supraoptic, and preoptic areas. By independent component analysis density segmentation and by interferential contrast, we identified GnRH non-neuronal positive bodies as microglial cells encapsulated within a dense halo of reaction products. These GnRH-positive microglial cells were distributed in patches and rows throughout the basal ventromedial hypothalamus, suggesting their role in paracrine or juxtacrine signaling. Moreover, as shown by ionized calcium-binding adaptor molecule 1 (IBA1) immunocytochemistry, the distribution of GnRH reaction products overlapped with the microglial dense reactive zones. Therefore, our findings support the assertion that a combined densitometric analysis of GnRH and IBA1 immunocytochemistry enables activity mapping for monitoring seasonal changes following experimental interventions.

## 1. Introduction

In sheep, behavioral and environmental factors, such as stress, seasonal light cycles and temperature fluctuations, induce changes in the estrus cycle. Referred to as hypothalamic activation, these changes require interactions between the hypothalamus-pituitary-adrenal axis and the hypothalamus-pituitary-ovarian axis for fertility regulation. This complex neuroendocrine process is triggered and regulated by gonadotropin releasing hormone (GnRH) synthesis and secretion into the pituitary portal blood flow [1].

GnRH stimulates the release of sex hormones during the estrous cycle, so variations in its levels must be analyzed to monitor the effects of environmental factors or hormonal treatments following fertility regulation experiments. Direct detection of GnRH in blood samples is not suitable for this purpose due to its episodic and pulsatile delivery and to its rapid removal and recycling [2–5]. Therefore, efforts have been made to directly analyze GnRH release from the portal vascular network using surgically implanted devices in the pituitary to extract blood samples [6].

Previous immunocytochemistry studies have assessed whether the cyclic estrous release of GnRH (before and during the LH surge and on day 8 and 15 of the subsequent luteal phase) is associated with morphological reorganization of GnRH-positive neurons in the hypothalamus of sheep by assessing the number and topography of neuronal somas [7]. But the distribution of these neurons throughout the brain is diffuse. So, the hypothalamic levels of secreted GnRH immunoreactivity must also be quantified to establish objective criteria for detecting changes in activation.

By Nissl staining and immunocytochemistry analysis of ionized calcium-binding adaptor molecule 1 (IBA1), glial fibrillary acidic

* Corresponding author.
*E-mail address:* carlospalacios@usal.es (C. Palacios).

https://doi.org/10.1016/j.theriogenology.2024.07.012
Received 22 March 2024; Received in revised form 29 June 2024; Accepted 15 July 2024
Available online 21 July 2024

protein (GFAP), and calcium-binding proteins in serial sections across three anatomical planes, we have recently characterized the morphology of basal hypothalamic nuclei related to sheep fertility [8]. In this study, we detected intense microglial immunoreactivity in the posterior, anterior, and preoptic hypothalamic areas, particularly in specific hypothalamic nuclei, such as the arcuate, paraventricular, suprachiasmatic, and supraoptic nuclei, and the reaction products were also diffusely distributed around the ventricles [8]. Criteria for glial cell activation, such as increased cell size, thickness, and branching [9,10], are widely met in periventricular areas of the hypothalamus. And while interactions between GnRH and glia are not yet fully elucidated, glial cells likely regulate GnRH synthesis and secretion [11–14] Accordingly, the microglial reactivity observed in our study may be related to GnRH hormonal feedback effects on the medio-basal hypothalamus [11,15, 16].

To test this hypothesis, the present study aims at analyzing potential cellular and topographical correlations between IBA1-positive cells (microglia) and GnRH immunoreactivity in the ventromedial hypothalamus. To this end, we analyzed the immunoreactivity of these markers in regions involved in seasonal fertility regulation (SFR) of the mediobasal hypothalamus, focusing on the posterior (Arcuate nucleus – ARC), anterior (Supraoptic nucleus – SO and Periventricular nucleus – PVN), and preoptic (POA) areas. Ultimately, our findings may shed light on the functional involvement of microglia in GnRH regulation while laying the groundwork for monitoring seasonal activation in the hypothalamus of ewes.

## 2. Materials and methods

### 2.1. Experimental groups

Six Churra ewes (age = 16.60 ± 0.25 months); mean live weight [(LW) = 70 ± 6 kg] housed under natural light, temperature, and humidity conditions, fed ad libitum and provided with unrestricted access to clean drinking water, were used in this study conducted in a farm. All experiments were performed in accordance with Spanish (RD 53/2013) and European (63/2010/EU) directives, and animal maintenance and care met all requirements of the agreement on the use of animals in scientific experimentation of the Confederation of Scientific Societies of Spain (*Confederación de Sociedades Científicas de España* – COSCE). Accordingly, the animals were sacrificed at the slaughterhouse MACRISA, in Medina de Rioseco, Valladolid, Spain, in April 2021, by neck cutting, severing the carotid and jugular veins, without prior drug administration. Heparinized 5-ml tubes were used to collect blood samples by jugular venipuncture, the samples were immediately centrifugated at 3000×*g* for 20 min, and plasma was stored at −20 °C.

Progesterone levels were measured in a single test using radioimmunoassay (RIA). Differences in progesterone levels show lack of estrous synchronization. Thus, only three of the six ewes with similar progesterone levels, from 15 to 20 mg/l, were selected to perform the techniques.

### 2.2. Animal samples

After removing the skin, the skull was cut horizontally from the external occipital protuberance to the upper edges of the orbits using an ultra-fast surgical saw with a radial disc 5 cm in diameter. Using this approach, the superficial dorsal area of the cortex was cleanly cut, exposing the ventricles in the midline while maintaining intact the diencephalic area. This procedure provided access to the ventricles for a faster and more effective fixation. After tilting the skull backwards with a spatula and a pair of tweezers, the brain was gently pushed to ventrally cut the optic nerves to release the brain rostrally and to reveal and cut the pituitary stem. Once cranial nerves and meningeal flanges were severed caudally, the brains shed and fell off under their own weight. The nerves were cut with a vise, and the meninges were removed from the pituitary stalk to facilitate infiltration of the fixative solution. The time elapsed from euthanasia to brain and pituitary fixation was approximately 5 min.

### 2.3. Histology

#### 2.3.1. Fixation and sectioning

Each brain was placed in a biosafety container with 1500 ml of 4 % paraformaldehyde in 0.1 M phosphate buffer, pH 7.4 at 4 °C. After 48 h, to prepare standardized anatomical planes, the brains were coronally cut from the optic chiasm to 1 cm caudally to the mamillary body. The resulting squared blocks contained almost the entire diencephalon. Block tissues were fixed for one more week, renewing the fixation solution every 48 h, and then immersed in solutions with increasing sucrose concentrations (from 20 to 100 %). Subsequently, the diencephalic blocks were carved to obtain standardized anatomical planes, serially sectioned in the coronal plane at 40 μm using a freezing microtome.

#### 2.3.2. Immunostaining

Alternate coronal serial sections were stained for IBA1 and GnRH (for details about the antibodies used in this study, see Table 1). Free-floating sections were sequentially washed with 0.05 M tris buffer saline, pH 7.6, followed by endogenous peroxidase inhibition by incubation in 10 % methanol +3 % H2O2 in 0.1 M PB for 10 min. Subsequently, the sections were washed in 0.1 M PB and 0.05 M TBS-Tx, pH 8.0, 0.3 % Triton X-100 (T9284 Sigma, St. Louis, MO, USA; TBS-Tx) and incubated with the corresponding primary antiserum (Table 1) for 48 h at 4 °C. Non-specific labeling was blocked using fetal calf serum (10 %). After washing three times in TBS-Tx, for 15 min, all sections were incubated with an anti-rabbit biotinylated secondary antibody (biotinylated anti-rabbit IgG H + L, BA-1000; Vector, Burlingame, CA, USA) at a 1:200 dilution in TBS-Tx for 120 min at room temperature. The sections were then washed with TBS-Tx and incubated for 180 min in avidin/biotin–peroxidase (ABC complex, Vectastain Standard ABC kit PK-4000; Vector, Burlingame, CA, USA) and further washed with TBS-Tx and subsequently with Tris-HCl, pH 8.0. Lastly, the sections were incubated in 3,3-diaminobenzidine tetrahydrochloride (DAB; D-9015; Sigma-Aldrich, St. Louis, MO, USA) with 0.006 % $H_2O_2$ to visualize the peroxidase reaction. Negative controls, processed without the corresponding primary antibody, confirmed immunostaining specificity in all cases. A BLASTp analysis of the 16-amino-acid epitope (NPTGPPAKKAISELPC) of the antibody against IBA1 used as immunogenic protein against the sheep genome was also performed in this study, indicating 92.86 % homology: Results for BLASTP against Sheep Oar_rambouillet_v1.0 [Proteins (Ensembl)] - Ovis_aries_rambouillet - Ensembl genome browser 108.

#### 2.3.3. Image analysis

Panoramic mosaics of entire sections of the brain were captured at selected interaural coordinates. Digital photomicrographs (mosaics) were taken under a Leica DMRB microscope equipped with 10× objectives (Leica Plan Apo). These mosaics were assembled using the "Virtual slice" module of Neurolucida 10.0 (MBF-Bioscience CX 9000, Williston, Vermont, USA), adjusting the microscope illumination source before each image capture by using a standardized grayscale range and a stepped density filter (11 levels; EO Edmund industrial optics-ref 32599,

**Table 1**
Primary antiserum.Characteristics of the antibodies and dilutions used in this study.

| Antigen | Dilution | Immunogen | Description |
|---|---|---|---|
| IBA 1 | Wako 019-19741 1:1000 | C-terminus of Iba l' (NPTGPPAKKAISELPC') | Polyclonal rabbit, Wako Cat # 019-19741, RRID: AB_839504 |
| GNRH | Merck AB1567 1:7500 | LHRH (Sigma) conjugated to thyroglobulin. | Polyclonal rabbit, Merck Cat # AB1567, RRID: AB_2110397 |

Karlsruhe, Germany). To measure the area and perimeter of the cells, photomicrographs of sections were processed using ImageJ 2.0 software and maximum entropy plug in. Density threshold segmentation analysis was automatically performed to construct densitometric maps by independent component analysis (ICA) [17,18]. This method separates an image into three independent and uncorrelated color channels, which are more effective than RGB component images for density changes recognition. For correspondence between colors and density values (0–254), the calibration bar was processed in parallel with the images for a consistent numeric - visual appreciation of changes between hypothalamic areas. Interferential contrast (Nomarsky analyisis) images were acquired using a ×40 pan-apochromatic objective under a Leica DMRB microscope.

## 3. Results

### 3.1. GnRH immunocytochemistry

We identified positive neurons, nerve fibers, encapsulated microglial cells and distinct areas of interstitial reactivity within the posterior, anterior, and POA regions of the hypothalamus. For clarity, we defined interstitial immunoreactive zones as superficial areas lacking positive cellular structures but displaying a denser immunoreaction, over the background staining levels. Although GnRH neurons are widely

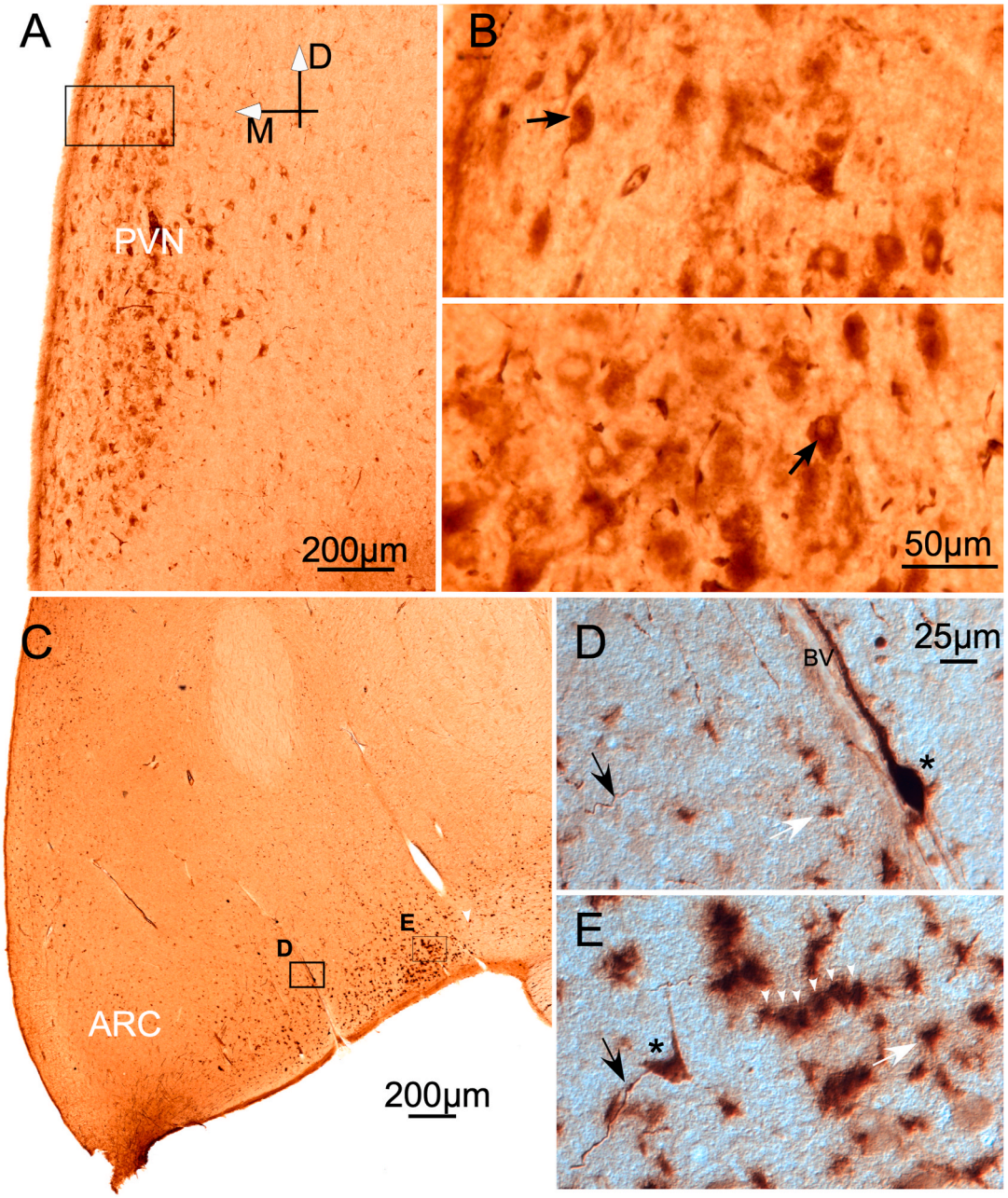


**Fig. 1.** GnRH immunocytochemistry in coronal serial sections (Mosaics).
A. Neuronal immunoreactivity in the anterior hypothalamus. PVN: paraventricular nucleus – magnocellular area. B. Details of immunoreactive neurons at a higher magnification. The reaction product is located in the cytoplasm with a higher perinuclear density (arrows). C. Labeling in the posterior hypothalamus shows periventricular and ventral immunoreactive fibers and positive bodies; ARC: Arcuate nucleus. D and E. Nomarsky optic microphotographs. Details of varicose fibers (arrows), isolated dense neurons (asterisks), and positive immunoreactive bodies identify microglial cells (white arrows) BV: Blood vessel. In E, six microglial cells are organized in a row (arrowheads).

distributed throughout the brain, including the olfactory bulb, diagonal band of Broca, and medial septum, among other areas [19], we focused on the preoptic terminal, preoptic-infundibular, and periventricular hypothalamic areas, in line with the aim and scope of this paper.

Immunopositive neurons, displaying medium-to-low immunoreactivity, were predominantly observed in the magnocellular nucleus of the PVN (Fig. 1A and B). These PVN neurons showed reaction products in both soma and dendrites. In coronal sections, these neurons had a bipolar or stellate shape (Fig. 1B). Their somas were approximately 120± 26 μm in perimeter and displayed denser immunoreaction products close to and around the nuclei (Fig. 1B, arrows). Furthermore, densely immunoreactive neurons were also scattered throughout the anterior and preoptic hypothalamus. These neurons were often found near the large ventral blood vessels (Fig. 1C and D - arrow, and 1E). Scattered interstitial neurons displayed well-defined contours attributed to their black positive immunoreaction products. Their sizes ranged from medium to large, and they had a fusiform or stellate shape, typically with thick, spiny dendrites (Fig. 1D and E).

Immunoreactive thin and varicose fibers were distributed along the preoptic and posterior periventricular surfaces, scattered along a band approximately 500 μm thick. These fibers converged, particularly in the arcuate and infundibular areas (black arrows in Fig. 1C and. D, and E).

Small, dense, immunoreactive patches were randomly distributed along a superficial band of approximately 400–500 μm in the preoptic and posterior periventricular areas (Fig. 1C). At low magnifications, these patches showed poorly defined borders, ranging from 15 μm to 150 μm in perimeter (Fig. 1C). However, when observed at higher magnifications under an interferential contrast optic (Nomarsky optic), small cells with radiant thin profiles were discerned and, thus, easily identified as microglial cells. We often observed rows and patches of these microglial cells, whose size varied with the reaction products they accumulated (compare white arrows between Fig. 1D and E). We also observed microglial positive bodies along the anterior hypothalamus and POA. However, these superficial microglial patches, intermingled with fibers, exhibited a significantly higher concentration in a peripheral external and periventricular band along the posterior hypothalamus (Fig. 2A–C). ICA pseudocolor imaging processing improved the visualization of GnRH immunoreactive areas (depicted in white or magenta), facilitating their differentiation from background staining (appearing brown-yellow) [20]. In ARC, MPO, and lateral retro-chiasmatic areas of

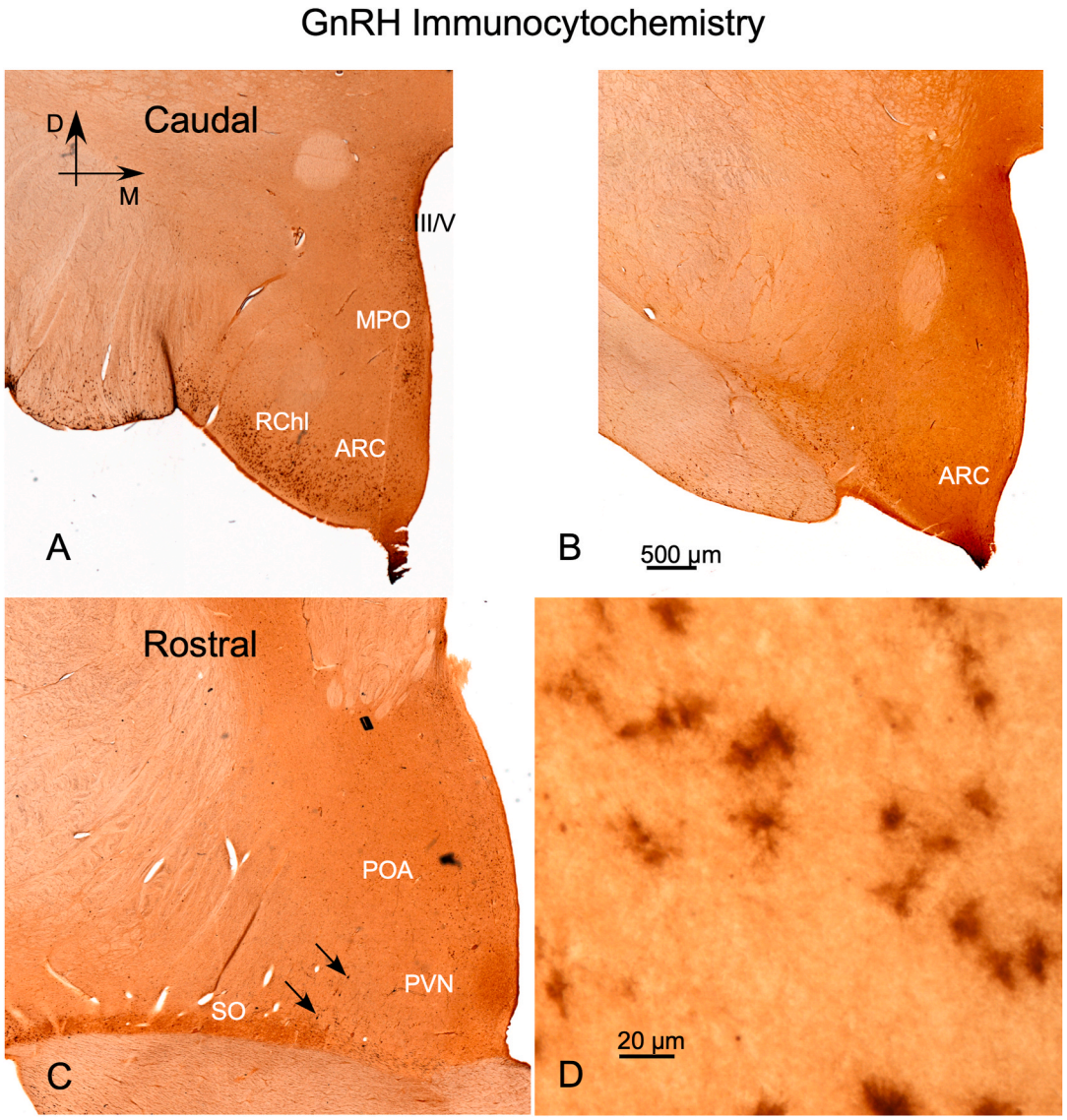


**Fig. 2.** Panoramic high-resolution mosaics showing GnRH immunoreactivity in the posterior (A) and anterior (B) hypothalamus (arrows point to dense dispersed dark neurons, as shown at a higher magnification in Fig. 1. D). (C). Detail of positive and reactive microglia at a higher magnification; RChL: retrochiasmatic area – lateral part; MPO: Medial Preoptic; ARC: Arcuate nucleus; PVN: paraventricular nucleus; SO: supra optic nucleus; POA: Preoptic area.

the posterior hypothalamus, microglial immunopositive bodies (Fig. 3A and B, arrowheads), as well as magenta diffuse dense immunoreactive areas bordered the juxtaventricular and ventral regions in contact with cerebrospinal fluid (Fig. 3A and B, asterisk) and the superficial interstitial perivascular spaces (Fig. 3, arrow). In the preoptic and anterior hypothalamus, as well as in POA, SO nucleus, and PVN, we observed a more intense magenta (supra-background threshold) reactivity, along with smaller and more dispersed microglial bodies than in caudal sections. Positive fibers were clearly visible within a diffuse magenta staining covering approximately 1.5 mm of the periventricular area (Fig. 3C). Furthermore, ICA segmentation confirmed that GnRH-positive bodies consist of ramified microglial cells, with the densest cell bodies shown in white (Fig. 3D), surrounded by a less dense magenta halo (Fig. 3D, arrow).

### 3.2. IBA 1 immunoreactivity

In regions outside the hypothalamus (not shown), IBA1-positive microglial cells typically exhibited small somas with 4 or 5 thin ramifications. However, in our regions of interest (posterior, anterior, and preoptic areas), IBA1-positive cells displayed denser somas and thicker prolongations (Inset in Fig. 4C). In these areas, hypothalamic nuclei were clearly defined by their dense reactive glial configuration. Immunoreactivity facilitated the identification of the boundaries of the largest

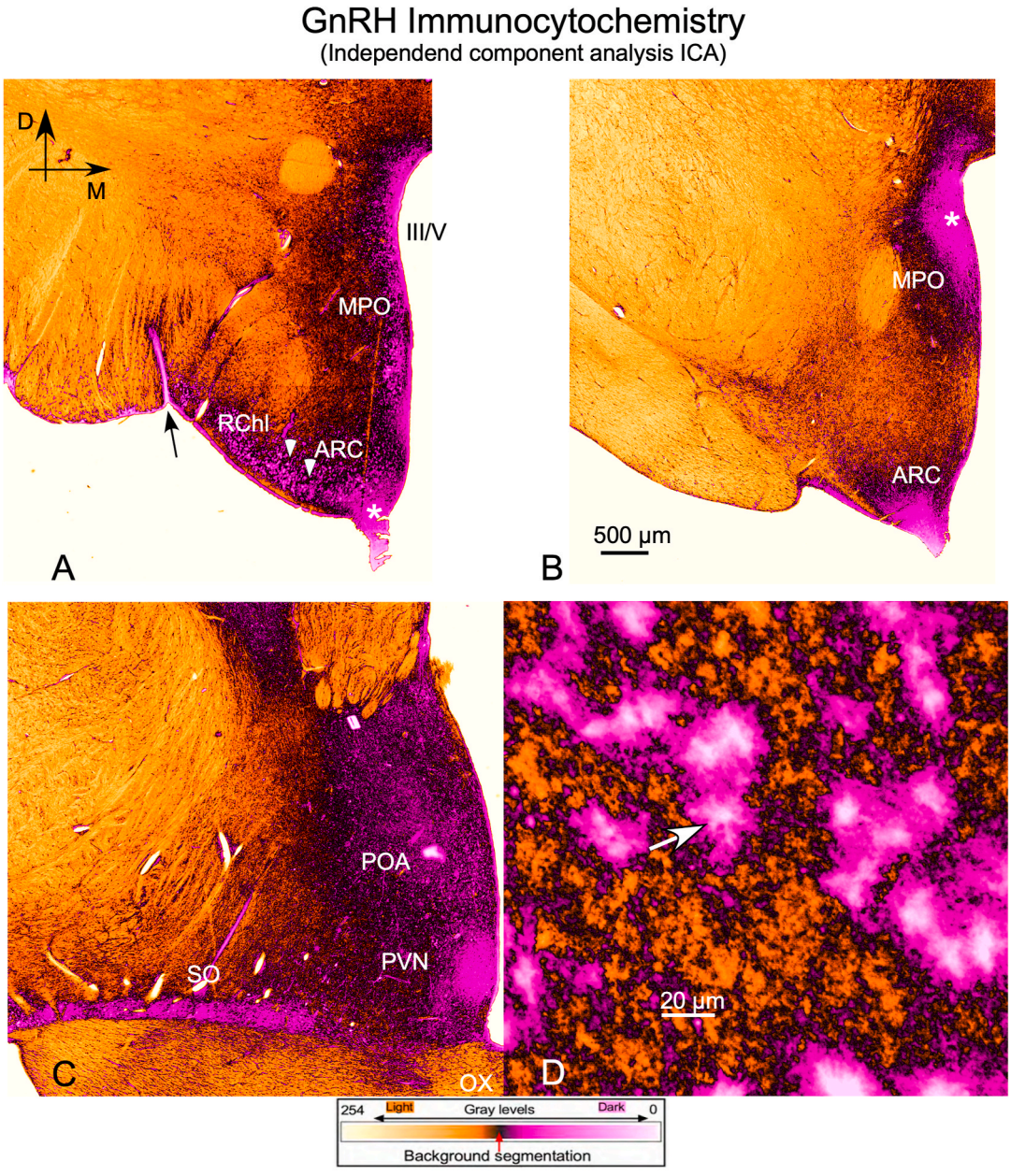


**Fig. 3.** Panoramic microphotographs shown in Fig. 2 after ICA pseudocolor image processing for mapping changes in GnRH reaction product density. The scale bar at the bottom defines the correspondence between grey scale values 0-254 and colors. White and magenta define the denser zones, whereas brown and yellow represent the background. The dark color in the middle of the scale corresponds to the density threshold of pseudocolor image processing. A and B show the densest reactivity in the posterior hypothalamus, including reactive microglial bodies, fibers, and neurons. The arrow in A points to an immunopositive blood vessel. C illustrates a diffuse and delimited area of reactivity in POA, with a higher density in neuronal nuclei. D - At a higher magnification, ICA image processing facilitates the definition of intense immunostained (white) microglial cells (white arrow) encapsulated within a GnRH-positive halo (magenta). (For interpretation of the references to color in this figure legend, the reader is referred to the Web version of this article.)

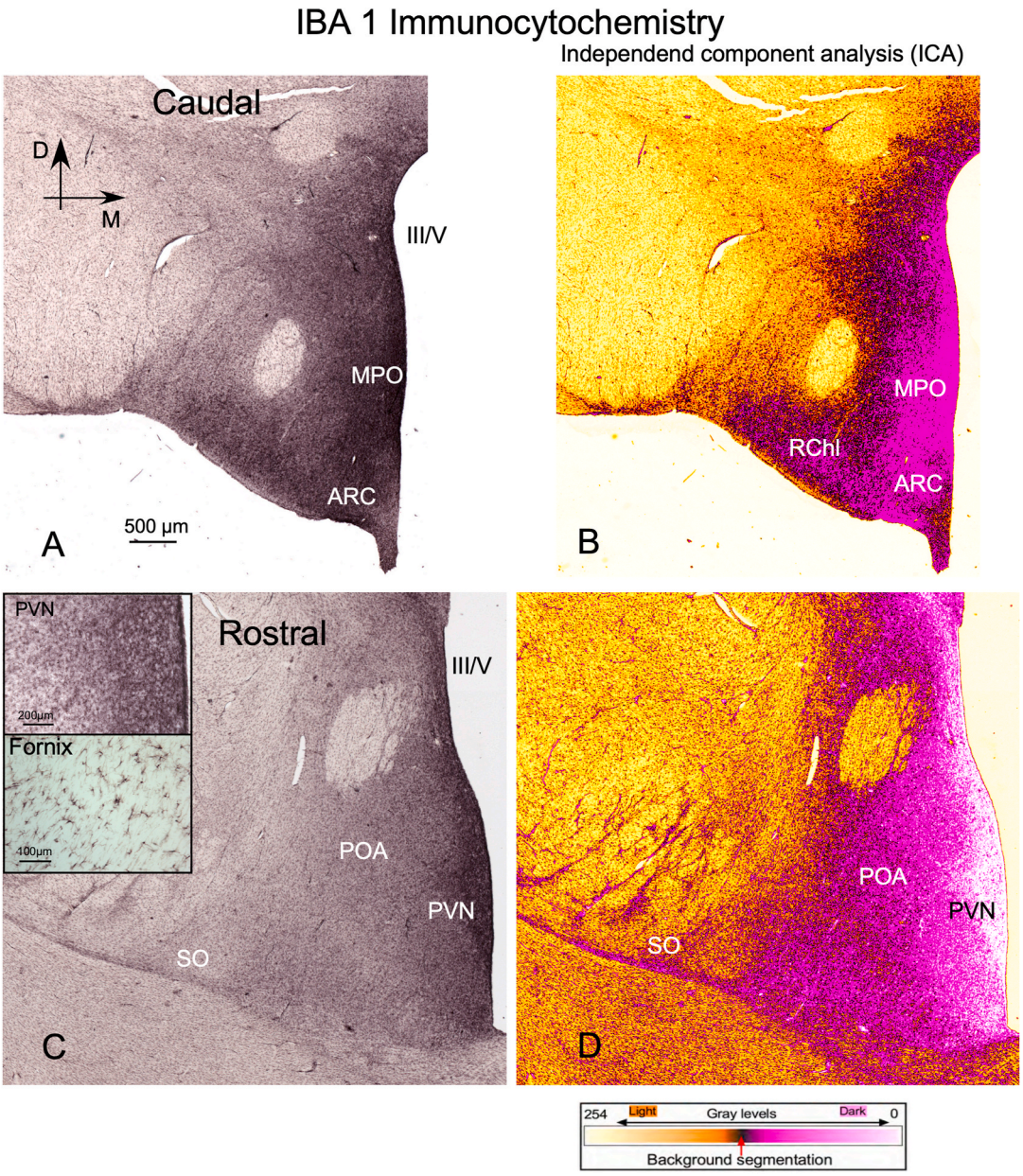


**Fig. 4.** IBA1 immunocytochemistry, panoramic views. A. Posterior hypothalamus showing microglial reactivity distributed along the ventromedial hypothalamus. B. ICA image processing highlights a higher glial reactivity around neuronal nuclei. C and D. Similar results are shown in the anterior and preoptic hypothalamic area. Inset. Details at a higher magnification of reactive microglia in and around PVN, and resting microglia in the Fornix, RChL: retrochiasmatic area – lateral part; MPO: Medial preoptic; ARC: Arcuate nucleus; PVN: paraventricular nucleus; SO: supraoptic nucleus; POA: Preoptic area.

nuclei, such as the retrochiasmatic or MPO in the posterior and SO or PVN in the anterior and supraoptic areas (Fig. 4). Nevertheless, ICA image processing revealed that the maximum density immunoreactivity in these principal nuclei (white) spreads out in all directions (magenta), covering almost the entire extension of the ventromedial hypothalamus (Fig. 4). In the preoptic hypothalamus, this method of analysis enabled us to define a clear border for POA and zona incerta, two areas commonly known for hampering a precise cytoarchitectural delimitation.

Although the densest GNRH immunostained areas generally topographically matched the areas of higher microglial reactivity in the periventricular, supraoptic, ARC and retrochiasmatic hypothalamus, IBA1 immunocytochemistry showed a more diffuse interstitial distribution (compare Figs. 3 and 4).

## 4. Discussion

In this study, we demonstrated a close topographical correlation between reactive microglial and GnRH immunoreactivity areas in the basal hypothalamus of ewes during the estrous period, highlighting functional activation during the natural mating and breeding season. With different cycles of gonadal activation, the natural fertility season of ewes typically spans from February to June when the levels of sex hormones significantly vary as a function of changes in HPA and HPO over time. To ensure standardization in such a period of high hormonal variability, we analyzed ewes euthanized in April, approximately at the midpoint of the seasonal fertility period, with blood levels of progesterone ranging from 15 to 20 mg/l [21].

GnRH immunocytochemistry was first described in the hypothalamus of rodents, such as guinea pigs [22], hamsters [23], and rats [24]. Yet, despite its well-known preoptic-terminal, preoptic-infundibular,

and periventricular pathways, GnRH showed a wide distribution of immunoreactive fibers in major tracts and areas of the brain (medial and cortical amygdaloid complex, stria terminalis, stria medullaris thalami, fasciculus retroflexus, medial forebrain bundle, stria longitudinalis medialis and lateralis, hippocampus, and periaqueductal grey of the mesencephalon) [24], indicating many potential extrahypothalamic sources outside the scope of this study. More recently, GnRH immunoreactivity has been extensively and carefully described in the hypothalamus of large ruminants such as sheep [22,23] and llamas [24]. As previously reported [25–27], we observed scattered, Golgi-like, GnRH-positive neurons along the preoptic area, in addition to larger neurons with medium-density immunoreactive products in PVN (Fig. 1A and B). The latter had a morphology similar to that described by Batailler et al. [28] (Fig. 4 in their study). In domestic pigs, ontogenic analysis revealed LHRH-positive perikarya in the most anterior periventricular parts of the hypothalamus, in the preoptic area, in the diagonal band of Broca, and seldom in the medial-basal hypothalamus. However, false-negative GnRH and peptide-positive neurons can be expected when performing immunocytochemical analysis, most likely due to the extremely fast transport and release of hormones and growth factors, according to previous authors [29]. For this reason, we performed pseudocolor image processing for determining not the neuronal synthesis alone, but the total amount of GnRh reaction products along the ventro-basal hypothalamus (fibers, interstitium and microglia).

After our ICA pseudocolor image processing, we detected higher concentrations of reaction products, with and without positive perikaria, overlapping with the main hypothalamic nuclei, such as PVN, MPO, ARC and SO nuclei (Fig. 3). These nuclei may thus correspond to areas of GnRH synthesis or delivery. Furthermore, the distribution of immunoreactive thin varicose fibers from the preoptic-terminal, mediobasal, and laterobasal pathways corroborated the findings of Caldany et al. [26].

Although the reaction product was detected in neuronal somas and fibers, we have also observed an interstitial distribution of positively dense, small-to-medium-sized bodies in the posterior hypothalamus (retrochiasmatic, ARC, and periventricular areas) and, in a lower concentration, in the preoptic region. After interferential contrast (Fig. 1D and E) and ICA pseudocolor image processing, these bodies were identified as densely immunopositive microglial cells surrounded by a less dense but, nevertheless, immune-positive halo (Fig. 3D, arrow), so our anatomical results support the hypothesis that reactive microglial cells in the hypothalamus promote the concentration and processing of GnRH. Accordingly, qualitative or quantitative analysis of GnRHand IBA1 immunoreactive microglia should be considered a marker of the state of hypothalamic activation.

Glial cells regulate many different neuronal functions by secreting bioactive molecules that induce an external paracrine-juxtacrine signaling modulating GnRH neurons [26]. These authors have demonstrated a close contact between astrocytes and GnRH cell bodies and processes. Contradicting the classical view that microglia are activated under pathological conditions, over the last decade, mounting evidence has demonstrated that microglia must be considered housekeeping cells with key functions in many neuronal functions. In the preoptic area of the sheep hypothalamus, triple-labeled immunofluorescent histochemistry has revealed that COX-1 around GnRH-positive cells was localized entirely in CD11b-ir cells, matching the morphology of ramified microglia in female rats [30]. However, in our material, GnRH-positive reactive microglia were extensively detected near positive neurons and in rows along immunoreactive fibers, supporting a direct juxtacrine function (rows in Fig. 1D and E, arrows). The overlapping hypothalamic distribution of reactive microglial cells (more diffuse) and GNRH-immunoreactive products (more delimited) (compare Figs. 3 and 4) may be understood as a mechanism of global clearing and cell processing of GNRH from the interstitium after paracrine diffuse secretion. Autocrine regulation of hypothalamic GNRH has been previously demonstrated in a study which showed that receptors are expressed in hypothalamic GnRH neurons and that receptor activation is required for pulsatile GnRH release *in vitro* [31]. Thus, microglial modulation of GnRH neurons through paracrine-juxtacrine signaling supports the anatomical overlap between areas of reactive microgliocytes and hypothalamic areas of GnRH synthesis [26]. Our working hypothesis is that estral hypothalamic activation can be measured by assessing microglial reactivity in GnRH-positive hypothalamic nuclei. As such, GnRH-positive dense bodies most likely are not artifacts, so their number, size, and distribution must be also analyzed to evaluate seasonal hypothalamic activation, regardless of the number of GnRH-positive neurons and fibers.

Our IBA1 immunocytochemistry results showed peripheral and periventricular reactive microglia in both the posterior and preoptic hypothalamus, confirming our previous findings [8]. The most relevant feature identified when comparing GnRH- and IBA1-immunostained sections was their overlapping distribution (compare ICA pseudocolor density in Figs. 3 and 4). Considering the typical morphology (density, size, and branching pattern) of glial cells in these overlapping areas, these cells are reactive microglia, with a widespread impact on neuronal and circuit function through physiological interactions [32]. Therefore, the evidence provided in this study facilitates a comprehensive evaluation of hypothalamic activation after seasonal changes in ewes.

In this article, we highlight the critical role of microglia in the regulation of gonadotropin-releasing hormone (GnRH) neurons. As the resident immune cells of the central nervous system, microglia are known to interact with GnRH neurons strongly, modulating their activity and, consequently, reproductive function. These interactions are particularly relevant in seasonal breeding animals, such as sheep, whose hypothalamic-pituitary-gonadal (HPG) axis undergoes substantial seasonal changes.

Microglia contribute to the regulation of GnRH through several mechanisms, including the secretion of cytokines, growth factors, and other signaling molecules that can modulate neuronal activity. In sheep, seasonal changes in photoperiod are transduced into neuroendocrine signals within the hypothalamus, ultimately activating or suppressing the HPG axis. As shown in this study, the correlation between reactive microglia and GnRH further supports the hypothesis that glial-neuron dialogue is a key mediator in this process as they respond to environmental cues and alter their functional state accordingly. This dynamic response allows microglia to either promote or inhibit GnRH neuron activity based on the season, thus regulating reproductive timing.

Understanding the role of microglia in GnRH regulation not only advances our knowledge of neuroendocrine control mechanisms but also lays a foundation to develop novel methods for monitoring and potentially controlling seasonal reproductive activation in sheep. By identifying specific microglial markers or signaling pathways associated with seasonal changes or interventions (e.g., photoperiod), we may predict or influence breeding cycles, with significant benefits for animal production practices.

## 5. Conclusions

Based on our immunocytochemistry analysis of the ventro-basal hypothalamic area of ewes during the estrous period, GnRH-positive microglial cells are dispersed along the periventricular and ventromedial surface, indicating a direct involvement of microglial juxtacrine signaling in gonadotropic seasonal fertility regulation. The topographical overlap of the densest IBA1-and GnRH- immunopositive areas in SFR nuclei and interstitium in POA and caudal hypothalamus, together with previous data on the role of microglia in GnRH regulation, supports the idea that microglial reaction is a good marker for hormone synthesis activation. The findings of this study provide valuable insights, enabling us to develop a suitable immunocytochemistry method for monitoring SFR by assessing key markers in the hypothalamus of ewes following experimental interventions. Overall, our results underscore the intricate interplay between GnRH, microglia, and the hypothalamic regions

involved in SFR in ewes, highlighting avenues for future research and potential applications in reproductive biology.

## Funding

This study was supported by the Spanish Ministry of Science and Innovation (Ministerio de Ciencia e Innovación – MICINN) Grant number: PID2020-117266RB-C21.

## CRediT authorship contribution statement

**M. Merchán:** Writing – original draft, Supervision, Software, Resources, Methodology, Investigation, Formal analysis, Data curation, Conceptualization. **I. Plaza:** Supervision, Methodology, Investigation. **J. Nieto:** Writing – review & editing, Visualization. **J. Plaza:** Writing – review & editing. **J.A. Abecia:** Writing – review & editing, Supervision. **C. Palacios:** Writing – review & editing, Writing – original draft, Supervision, Resources, Methodology, Investigation, Formal analysis, Conceptualization.

## Acknowledgments

We would like to thank Carlos V. Melo for editing the manuscript.

## References

[1] Dobson H, Routly JE, Smith RF. Understanding the trade-off between the environment and fertility in cows and ewes. Anim Reprod 2020;17(3):1–30.
[2] Evans NP. Pituitary portal blood : a history 2022;34(5).
[3] Clarke IJ, Thomas GB, Yao B, Cummins JT. GnRH secretion throughout the ovine estrous cycle. Neuroendocrinology 1987;Jun;46(1):82–8.
[4] Krsmanovic LZ, Hu L, Leung PK, Feng H, Catt KJ. The hypothalamic GnRH pulse generator: multiple regulatory mechanisms. Trends Endocrinol Metabol 2009;20:402–8.
[5] Izzi-Engbeaya C, Abbara A, Cass A, Dhillo WS. Using aptamers as a novel method for determining GnRH/LH pulsatility. Int J Mol Sci 2020;21(19):1–15.
[6] Caraty Alain, Locatelli Alain, Suzanne M, Moenter FJK. Sampling of hypophyseal portal blood of conscious sheep for direct monitoring of hypothalamic neurosecretory substance. Methods Neurosci 1994;20:162–83.
[7] Batailler M, Caraty A, Malpaux B, Tillet Y. Neuroanatomical organization of gonadotropin-releasing hormone neurons during the oestrus cycle in the Ewe. BMC Neurosci 2004;5:1–8.
[8] Jr MM, Coveñas R, Plaza I, Abecia JA, Palacios C. Anatomy of hypothalamic and diencephalic nuclei involved in seasonal fertility regulation in ewes. (4).
[9] Stence N, Waite M, Dailey ME. Dynamics of microglial activation: a confocal time-lapse analysis in hippocampal slices. Glia 2001;33(3):256–66.
[10] Banati RB. Visualising microglial activation in vivo. Glia 2002;40(2):206–17.
[11] Adachi S, Fujioka H, Kakehashi C, Matsuwaki T, Nishihara M, Akema T. Possible involvement of microglia containing cyclooxygenase-1 in the accumulation of gonadotrophin-releasing hormone in the preoptic area in female rats. Neuroendocrinology 2009;15:1029–37.
[12] Sharif A, Baroncini M, Prevot V. Role of glia in the regulation of gonadotropin-releasing hormone neuronal activity and secretion. 2013. p. 1–15.
[13] Fujioka H, Kakehashi C, Funabashi T, Akema T. Immunohistochemical evidence for the relationship between microglia and GnRH neurons in the preoptic area of ovariectomized rats with and without steroid replacement Endocrine. Journal 2013;60(2):191–6.
[14] Ojeda SR, Lomniczi A, Sandau US. Glial-gonadotrophin hormone (GnRH) neurone interactions in the median eminence and the control of gnrh secretion. J Neuroendocrinol 2008;20(6):732–42.
[15] Fujioka H, Kakehashi C, Funabashi T, Akema T. Immunohistochemical evidence for the relationship between microglia and GnRH neurons in the preoptic area of ovariectomized rats with and without steroid replacement 2013;60(2):191–6.
[16] Sharif A, Baroncini M, Prevot V. Role of glia in the regulation of gonadotropin-releasing hormone neuronal activity and secretion. Neuroendocrinology 2013;98(1):1–15.
[17] Tailor DR, Finkel LH, Buchsbaum G. Color-opponent receptive fields derived from independent component analysis of natural images. Vis Resour 2000;40(19):2671–6.
[18] Liu C, Yang J. ICA color space for pattern recognition. IEEE Trans Neural Network 2009;20(2):248–57.
[19] Merchenthaler I, Göres T, Sétáló G, Petrusz P, Flerkó B. Gonadotropin-releasing hormone (GnRH) neurons and pathways in the rat brain. Cell Tissue Res 1984;237(1):15–29.
[20] Carmona-Barrón VG, Fernández del Campo IS, Delgado-García JM, De la Fuente AJ, Lopez IP, Merchán MA. Comparing the effects of transcranial alternating current and temporal interference (tTIS) electric stimulation through whole-brain mapping of c-Fos immunoreactivity. Front Neuroanat 2023;17(March):1–17.
[21] Caraty A, Skinner DC. Progesterone priming is essential for the full expression of the positive feedback effect of estradiol in inducing the preovulatory gonadotropin-releasing hormone surge in the Ewe. Endocrinology 1999;140(1):165–70.
[22] Silverman AJ, Krey LC, Rockefeller T, Silverman AJ, Krey LC. Department of anatono, columbia university (U.S.A.) (Accepted March 9th, 1978)157. New York, N. Y.: College of Physicians and Surgeons and The Rockefeller University; 1978. p. 233–46.
[23] Jennes L, Stumpf WE. LHRH-systems in the brain of the golden hamster. Cell Tissue Res 1980;209(2):239–56.
[24] Merchenthaler I, Petrusz P, Hill C. andTissue research, 9; 1984. p. 15–29.
[25] Lehman MN, Robinson JE, Karsch FJ, Silverman A-J. Immunocytochemical localization of luteinizing hormone-releasing hormone (LHRH) pathways in the sheep brain during anestrus and the mid-luteal phase of the estrous cycle. J Comp Neurol 1986;244(1):19–35.
[26] Caldani M, Batailler M, Thiéry JC, Dubois MP. LHRH-immunoreactive structures in the sheep brain. Histochemistry 1988;89(2):129–39.
[27] Carrasco RA, Singh J, Adams GP. Distribution and morphology of gonadotropin-releasing hormone neurons in the hypothalamus of an induced ovulator – the llama (Lama glama). Gen Comp Endocrinol [Internet] 2018;263(March):43–50. https://doi.org/10.1016/j.ygcen.2018.04.011.
[28] Batailler M, Caraty A, Malpaux B, Tillet Y. Neuroanatomical organization of gonadotropin-releasing hormone neurons during the oestrus cycle in the Ewe, 8; 2004. p. 1–8.
[29] Nunemaker CS, Satin LS. Episodic hormone secretion: a comparison of the basis of pulsatile secretion of insulin and GnRH. Endocrine 2014;47(1):49–63.
[30] Fujioka H, Kakehashi C, Funabashi T, Akema T. Immunohistochemical evidence for the relationship between microglia and GnRH neurons in the preoptic area of ovariectomized rats with and without steroid replacement. Endocr J 2013;60(2):191–6.
[31] Krsmanovic LZ, Martinez-Fuentes AJ, Arora KK, Mores N, Navarro C, chen Hao-Chia, Stojilkovic S, Katt AJ. Autocrine regulation of gonadotropin-releasing hormone secretion in cultured hypothalamic neurons. Endocrinology 1999;140:No3.
[32] Morrison H, Young K, Qureshi M, Rowe RK, Lifshitz J. Quantitative microglia analyses reveal diverse morphologic responses in the rat cortex after diffuse brain injury. Sci Rep 2017:1–12. https://doi.org/10.1038/s41598-017-13581-z [Internet].